Temperature and injection dependence of the Shockley–Read–Hall lifetime in electron irradiated *n*-type silicon

H. Bleichner,[a] P. Jonsson,[b] N. Keskitalo, and E. Nordlander[c]
Scanner Laboratory, Department of Technology, Uppsala University, P.O. Box 534, S-751 21 Uppsala, Sweden

(Received 30 October 1995; accepted for publication 8 March 1996)

Using three measurement techniques the injection and temperature dependence of the Shockley–Read–Hall (SRH) carrier lifetime was studied. Flying-spot scanning was used for the measurement of lifetimes under low-level injection. Open-circuit carrier decay for the measurement of high-injection lifetime, and deep-level transient spectroscopy for the characterization of active recombination centers. The samples were silicon p-i-n type diodes (p^+-n-n^+) irradiated with 15 MeV electrons for lifetime control. The measurements consistently show that two defect levels located at $E_c-0.164$ eV ($E1$) correlated to the vacancy-oxygen complex and $E_c-0.421$ eV ($E4$) correlated to the single-negatively charged state of the divacancy are significant for the SRH lifetime in different injection domains in the low-doped n-type region. The $E1$ recombination center is dominating the high-injection lifetime and the $E4$ center is dominating the low-injection lifetime. Similar to other authors, additional defect levels have also been observed, but the $E1$ and $E4$ levels seem sufficient to explain the behavior of electron-irradiated semiconductor power devices.
 [S0021-8979(96)03912-6]

I. INTRODUCTION

The carrier lifetime is a transport parameter of significance in all electronic devices. In particular, the switching characteristics are highly linked to carrier lifetime. In most cases the minority carrier lifetime is sufficient. This goes especially for devices under low-level injection. In high-injection devices, however, switching characteristics traverse different domains of injection conditions. In each of these domains the carrier lifetime may be composed of combinations of recombinational effects. In the low-level injection domain, assuming a single dominant recombination center near the mid-band-gap energy the recombination process is straightforward, and it may be well described simply by means of the minority-carrier lifetime. In the moderately high injection domain, the recombination process is not only governed by the minority carriers, but has to account for majority carriers as well. For space-charge neutrality conditions the recombination may be characterized by the sum of electron and hole lifetimes, thus increasing the carrier lifetime substantially. In the very high injection domain, recombination is set by an Auger process reducing the carrier lifetime strongly with increasing injection level.

From the fairly simple physics outlined above, one may predict the switching behavior of e.g., a power device, and this is the way it is normally done in device simulation software. However, in the present paper it is shown that this kind of simple combinational physics does not work for silicon devices which are lifetime controlled by electron irradiation.

[a]Also at ABB Corporate Research, Dept. G, c/o IMC, P.O. Box 1084, S-164 12 Kista, Sweden.
[b]Also at Bofors Underwater Systems AB, SUTEC, P.O. Box 7073, S-580 07 Linköping, Sweden.
[c]Also at Univ. College of Gävle-Sandviken, S-801 76 Gävle, Sweden.

II. EXPERIMENT

The samples used in this study were p^+-n-n^+ diodes manufactured on commercially available neutron transmutation doped (NTD) n-type silicon. The nominal resistivity of the n base of the two sample types were 40 Ω cm and 110 Ω cm. These resistivities correspond to doping levels of approximately 1×10^{14} cm^{-3} and 4×10^{13} cm^{-3}, respectively. The samples are similar to p-i-n type power diodes, but the results of the measurements should be applicable to any sample undergoing transitions between different injection domains. The p^+ region was diffused to a depth of about 80 μm in the first case, and the p^+ and n^+ regions in the second case ranged to a depth of 15 μm, approximately. The diodes were irradiated for lifetime control with 15 MeV electrons, and annealed in an air ambient at 200 °C for 4 h.

In order to obtain the Shockley–Read–Hall (SRH) lifetime under low-level injection, an optical technique developed for the local and simultaneous determination of minority-carrier lifetime and resistivity was used. The technique, which is called the flying-spot scanning (FS) technique is outlined briefly here, and a full description is given elsewhere.[1] The reverse-biased p^+-n-n^+ diode is illuminated at the n^+ region by means of a low-power sinus-modulated excitation light source. Normally, this is a red light HeNe laser, shallowly generating a low concentration of electron-hole pairs. Only the holes, i.e., the minority carriers, contribute to the photocurrent after carrier diffusion through the n-type bulk towards the depletion region. The amplitude and phase of the generated photocurrent relative to the light-source sinewave are measured vs reverse-bias voltage. In this way, the minority-carrier lifetime and resistivity (intrinsic mobility) may be extracted. The FS instrument is elaborated in order to facilitate temperature variations in the sample between room temperature and 200 °C. Thus, the

 0021-8979/96/79(12)/9142/7/$10.00

temperature dependence of the low-injection minority-carrier lifetime may be investigated.

The high-injection lifetime was also measured by an optical technique. This technique is called the open-circuit carrier decay (OCCD) which is based on the more commonly known free-carrier absorption (FCA) technique where time- and space-resolved excess-carrier concentrations are measured at different injection levels. The OCCD technique is described in detail elsewhere.[2,3] The forward current supplies the n-base of the p-i-n type diode with excess carriers, and when the outer circuit is broken the excess carrier is subject to diffusion and recombination. This is all similar to the well-known open-circuit voltage (OCVD) technique.[4] Probing the carriers locally by means of a light beam and using the classical semiconductor continuity equation, a simultaneous extraction of the ambipolar carrier lifetime and the ambipolar diffusion coefficient for various high-injection levels may be performed. Facilities for the variation of the sample temperature were included in the instrument.

Hence, means were available to measure carrier lifetimes vs carrier injection and temperature ranging from low to very high injection levels from room temperature to an elevated temperature of ~200 °C.

The defects created by electron irradiation were electrically characterized using deep-level transient spectroscopy (DLTS).[5] The concentration and electrical properties of the electron-induced defect levels, i.e., recombination centers, were investigated.

III. EXPERIMENTAL RESULTS

A. Low-injection SRH lifetime

In order to investigate the influence caused by the electron irradiation on the semiconductor material, samples of two different n-base doping concentrations have been investigated. In this work, the samples doped to 1×10^{14} cm^{-3} (40 Ω cm) and 4×10^{13} cm^{-3} (110 Ω cm) are denoted as samples 1 and 2, respectively. The electron dose used for lifetime reduction in the samples were 2×10^{13} cm^{-2} for sample 1 and 5×10^{12} cm^{-2} for sample 2, approximately.

The minority-carrier lifetimes at room temperature measured by means of the FS technique in samples 1 and 2 were about 2.8 and 12 μs, respectively. In Figs. 1 and 2, the temperature dependence of the low-injection lifetime is shown. The measurements ranged between 300 and 420 K, and Figs. 1 and 2 correspond to samples 1 and 2, respectively. Measured values are represented by triangular markers in those figures.

In order to verify the significance of other defect levels than the ''near mid-gap'' level, DLTS was used to monitor the defect spectrum, cf. Fig. 3. Thus, among other defects—viz. $E1$, $E2$, and $E6$—the single-negatively charged state of the divacancy named $E4$ located at $E_c-0.421$ eV was observed (see Fig. 3). This is well in accordance with Ref. 6. Since two recombination centers, viz. $E1$ and $E4$, have been found to be sufficient when computing the carrier lifetimes vs the excess-carrier concentration and temperature, only these two independent defects have been included for the calculation of the low-injection lifetime in an n-type sample.

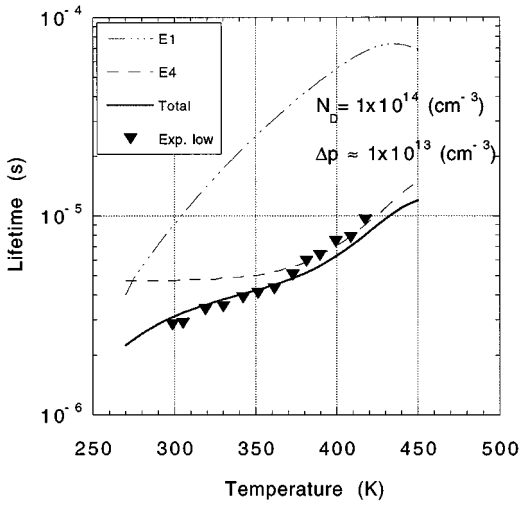

FIG. 1. Measured and computed low-injection effective lifetime in the n-region of diode 1 vs temperature. The experimental results are represented by markers (▼) and the computed total effective lifetime from the DLTS data by a solid line (—). The calculated lifetime of recombination center $E1$ (-·-), and $E4$ (---) are also included. Δp represents the approximately computed hole-carrier concentration generated by the low power excitation light source.

A more extensive description of these centers is presented in Sec. IV.

The following equations may be used according to[7]

$$\frac{1}{\tau}=\sum_{i=1}^{2}\frac{(\Delta n+n_0)}{\tau_{p_{0,i}}\times(\Delta n+n_0+n_i)+\tau_{n_{0,i}}\times(\Delta p+p_0+p_i)}, \quad (1)$$

$$\tau_{n_{0,i}}=\frac{1}{c_{n,i}\times N_{T,i}}, \quad (2)$$

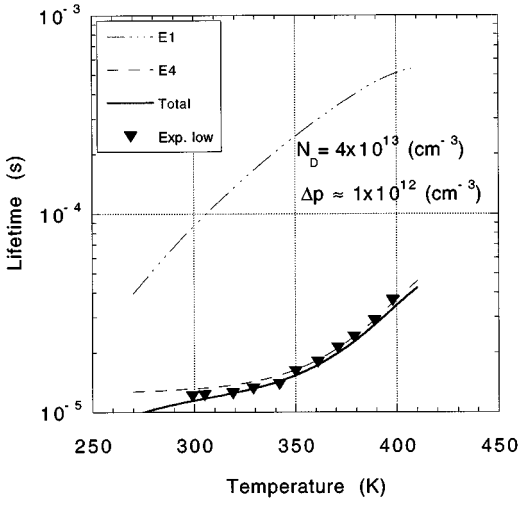

FIG. 2. Measured and computed low-injection effective lifetime in the n-region of diode 2 vs temperature. The experimental results are represented by markers (▼) and the computed total effective lifetime from the DLTS data by a solid line (—). The calculated lifetime of recombination center $E1$ (-·-), and $E4$ (---) are also included. Δp represents the approximately computed hole-carrier concentration generated by the low power excitation light source.

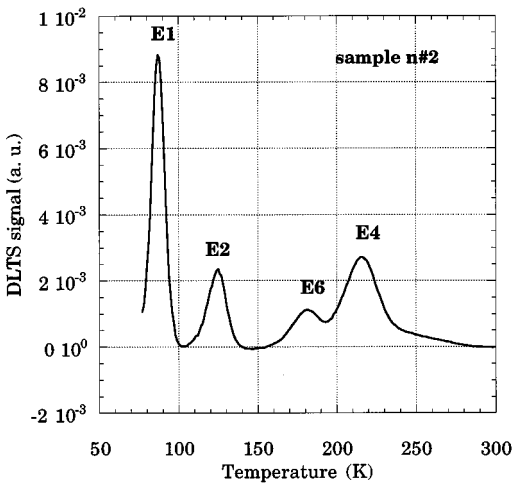

FIG. 3. DLTS spectrum for a sample of type 2. The sample was irradiated for lifetime control with 15 MeV electrons, and annealed in air ambient at 200 °C for 4 h.

$$\tau_{p_{0,i}} = \frac{1}{c_{p,i} \times N_{T,i}}, \tag{3}$$

where

$$n_i = N_c \times X_{n,i} \times \exp\left(- \frac{E_c - E_{t,i}}{kT} \right), \tag{4}$$

$$p_i = N_v \times X_{p,i} \times \exp\left(- \frac{E_{t,i} - E_v}{kT} \right). \tag{5}$$

$\tau_{n_{0,i}}$ and $\tau_{p_{0,i}}$ are the electron and hole minority-carrier lifetimes for a specific trap, respectively; n_0 and p_0 are the thermal equilibrium concentrations of electrons and holes; Δn and Δp are the excess electron and hole concentrations, where $\Delta n \approx \Delta p$ holds true under space-charge neutrality conditions; $N_{T,i}$ is the trap concentrations; $c_{n,i}$ and $c_{p,i}$ are the defect capture coefficients for electrons and holes, respectively; N_c and N_v are the effective densities of states in the condition and the valence band; and $X_{n,i}$ and $X_{p,i}$ are the entropy factors for electrons and holes, respectively.

Since Kimerling *et al.*[8,9] demonstrated that the defects created by proton irradiation are similar to those of electron irradiation, the capture coefficients ($c_{n,i}$,$c_{p,i}$) and entropy factors ($X_{n,i}$,$X_{p,i}$) for electrons and holes proposed by Hallén *et al.*[10] have been partly used in this investigation with correction (cf. Table I). The position of the recombination centers in the band diagram given in Table I, has been kept constant in relation to the conduction-band edge for all temperatures in this work.

In addition to the computed effective low-injection lifetime denoted ''Total'' in Figs. 1 and 2, two curves are drawn named ''$E1$'' and ''$E4$'' representing the calculated contribution of the respective trap.

From the equations above, Table I, and Figs. 1 and 2, it can be seen that the temperature behavior of the SRH minority-carrier lifetime ($\tau_{p_{0,E4}}$), is partly controlled by the temperature dependence of the capture coefficient of holes ($c_{p,E4}$), and by the temperature dependence of the Fermi level in the band diagram.

From the DLTS measurements demonstrated in Fig. 3 and measured low-injection lifetime values, the approximate $E4$ trap concentration ($N_{T,E4}$) was estimated to 9.5×10^{11} cm^{-3} in sample 1, and to 2.5×10^{11} cm^{-3} in sample 2. These values should be compared with the DLTS-obtained values of about 1×10^{12} cm^{-3} for sample 1 and 3×10^{11} cm^{-3} for sample 2 within the uncertainty of 20%. This procedure was used when estimating all needed value of trap concentrations. In Figs. 1 and 2, the agreement between measured and calculated lifetimes is striking.

B. High-injection SRH lifetime

The high-injection lifetimes in samples 1 and 2 were measured by a technique based on free-carrier absorption (FCA) of infrared light. This special case of FCA is called the open-circuit carrier decay (OCCD).[2,12]

According to the literature, the expected high-injection lifetime (τ_{HL}) for the case of a single recombination center is[6]

$$\tau_{HL} = \tau_{n_0} + \tau_{p_0} = \frac{1}{c_n \times N_T} + \frac{1}{c_p \times N_T}. \tag{6}$$

Moreover, the ratio of lifetimes for electron-irradiated samples according to Ref. 6 is $\tau_{n_0}/\tau_{p_0} = 4.2$. Equation (6) theoretically yields a lifetime 5.42 times higher in the high-injection regime than in the low-injection regime. Keeping this in mind, the measured results were surprising. The measured high-injection lifetime value was in the same range as the low-injection value, thus setting the commonly acknowledged fact of Eq. (6) aside.

An inspection of the DLTS defect spectrum of both sample types (samples 1 and 2) shows that three defect levels

TABLE I. Energy levels, entropy factors, and capture coefficients for electron and hole to electron traps, created in *n*-type silicon by irradiated 15 MeV electrons. The results are on the one hand deduced from DLTS measurements and on the other hand corrected by lifetime measurements. Temperature dependencies for the capture coefficients is given in degrees Kelvin.

Defect	Position [eV]	Entropy X_n	Capture coeff. Electrons, c_n [cm^3/s]	Capture coeff. Holes, c_p [cm^3/s]	Temperature interval [K]
$E1$	$E_C-0.164$	0.29	$6.4\times10^{7}\times\exp(-\frac{T}{150})$	$8\times10^{-8}\times T^{0.7}$	···
$E2$	$E_C-0.225$	4.6	$1.6\times10^{-12}\times T^{1.4}$	7×10^{-7}	105–155
$E4$	$E_C-0.421$	0.33	$5.4\times10^{-9}\times T^{0.4}$	$2\times10^{-6}\times T^{-0.3}$	182–266
$E6$	$E_C-0.35$	2	$2\times10^{-10}\times T^{0.7}$	···	167–223

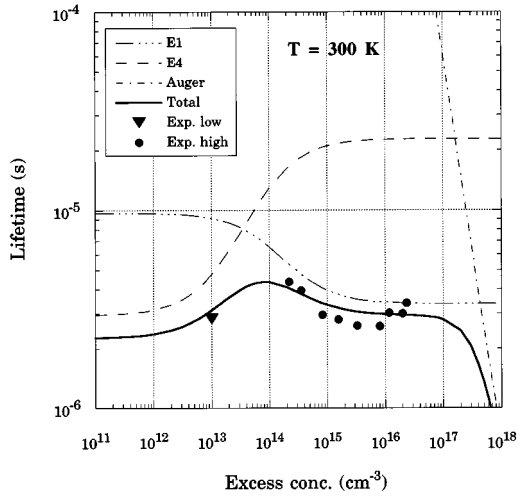

FIG. 4. The calculated room temperature total effective lifetime (—), the lifetime of the recombination centers $E1$ (-·-), and $E4$ (---) of sample 1 are shown vs excess-carrier concentration. The measured high-injection lifetimes for different excess-carrier concentrations are represented by (●). In the left part of the graph, the measured low-injection lifetime value is included (▼).

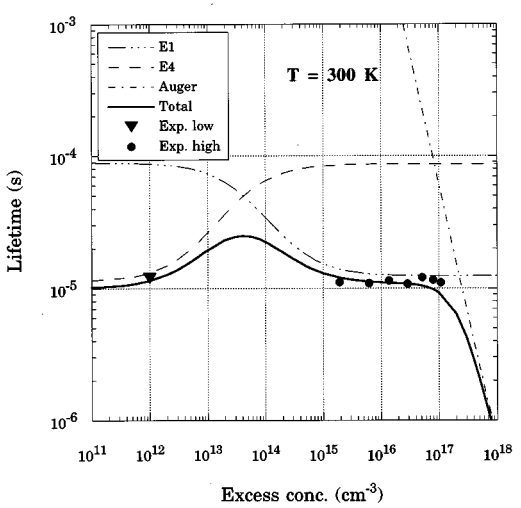

FIG. 5. The calculated room temperature total effective lifetime (—), the lifetime of the recombination centers $E1$ (-·-), and $E4$ (---) of sample 2 are shown vs excess-carrier concentration. The measured high-injection lifetimes for different excess-carrier concentrations are represented by (●). In the left part of the graph, the measured low-injection lifetime value is included (▼).

apart from the $E4$ level are possibly acting as efficient recombination centers (cf. Fig. 3), viz. $E1$ and $E2$, and a defect level $E6$ indicated by a response peak located immediately to the left of the $E4$ response peak. This result should indicate similarities with the behavior of proton-induced defects.[10] The recombination center $E6$ is not giving strong influence on the total effective lifetime in this work. This is due to the specific annealing process used for the investigated samples. However, for samples annealed at higher temperatures and longer annealing times than were used in this work, the $E6$ level will become more important and the $E4$ level tends to be annealed out.[11]

The influence of the $E2$ level is also negligible, which will be discussed in Sec. IV. For the $E1$ defect level, capture coefficients (c_n, c_p) and entropy factors (X_n, X_p) for electron and holes are also proposed by Hallén *et al.*[10] These values were used in this investigation (cf. Table I).

The concentration ratio of the defect levels, $N_{T,E1}/N_{T,E4}$, was found to be about 3.7 for sample 1 where $N_{T,E1} = 3.5 \times 10^{12}$ cm^{-3}, and the corresponding concentration ratio for sample 2 was estimated to 3.8 where $N_{T,E1} = 9.5 \times 10^{11}$ cm^{-3} (9.5×10^{11} cm^{-3} by DLTS). The total effective high-injection lifetime may be calculated combining Eqs. (1)–(5) and using the parameter values represented in Table I.

In Figs. 4 and 5, the calculated lifetimes of the recombination centers $E1$ and $E4$ of samples 1 and 2, respectively, at room temperature are shown vs excess-carrier concentration. Furthermore, the total effective lifetimes of samples 1 and 2 at room temperature were computed by means of the $E1$ and $E4$ data. The measured lifetimes for different injections levels, i.e., excess-carrier concentrations, are included. For clarity, in the left part of the respective graph, the measured low-injection lifetime value is put in. Inspecting the contributions from each defect level to the total effective lifetime, the dominating recombination center at high-injection levels is found to be $E1$. The explanation is that the $E1$ recombination center becomes more active as the electron quasi-Fermi level moves closer to the $E1$ defect level in the band diagram. This happens when the device goes into high-injection mode. The experimental results confirm this theory.

At higher temperatures, viz. 360 and 420 K, the agreement between measured and computed lifetimes is not equally satisfactory. The deviation of the measured data and the computed ones is most possibly due to the fact that the electron capture cross section (σ_n) for $E1$ was measured by DLTS techniques in the temperature interval of 80–108 K and extrapolated to room temperature and above. This extrapolation is somewhat provocative due to the large extrapolation range. This is illustrated in the left part of Fig. 6.

In Fig. 6, the $E1$ electron capture cross section proposed by Hallén *et al.*[10] is computed and represented by the thin line. In principle, its temperature behavior is almost constant. Furthermore in Fig. 6, an attempt to correct the σ_n value for higher temperatures is included. This was performed using lifetime measurements obtained by means of the OCCD technique.[12] Since the total effective high-injection lifetime with a reasonable precision is found to be controlled by the $E1$ electron lifetime τ_{n_0}, the σ_n can be computed from the relationship

$$\tau_{n_0} = \frac{1}{c_n \times N_T} = \frac{1}{\sigma_n \times v_{th} N_T}, \tag{7}$$

where v_{th} is the thermal velocity of electrons. For the calculation of v_{th} in this work, the electron rest-mass temperature dependence proposed by Green[13] has been used. For simplicity, the capture coefficient of electrons instead of the capture cross section is presented here. Thus, the obtained capture coefficient of electrons, c_n, and its temperature dependence valid in the 250–450 K interval is expressed by:

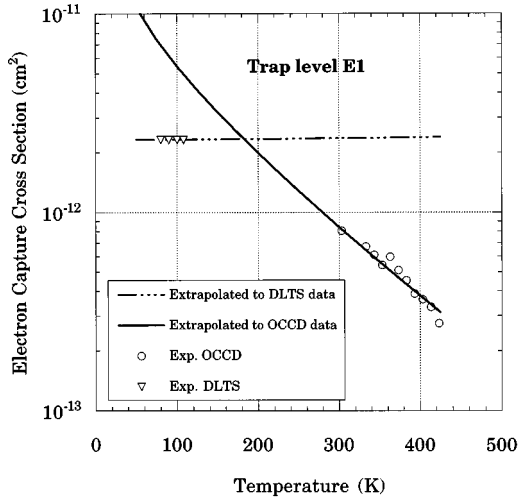

FIG. 6. Electron capture cross section, σ_n, of the recombination center $E1$ vs temperature. The experimental results in the corresponding temperature intervals of the DLTS (∇), and the OCCD ($\bigcirc$) are shown in the graph. The lines represent their respective extrapolation.

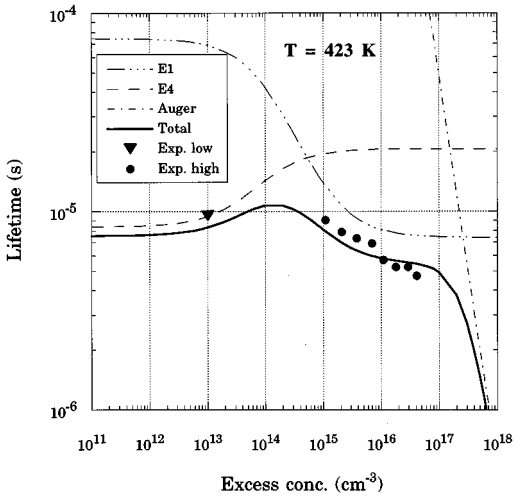

FIG. 8. The total effective lifetime of diode 1 vs excess carrier concentration at 423 K. The markers, (▼) and the (●) represent the measured low-, and the high-injection lifetime respectively. The solid line (—) shows the computed total effective lifetime from the DLTS data.

$$c_n = 6.4\times 10^{-7}\times \exp(-T/150) \qquad (\mathrm{cm}^3/\mathrm{s}). \tag{8}$$

In Figs. 7 and 8 for sample 1 and Figs. 9 and 10 for sample 2, the measured and calculated effective low-injection and high-injection lifetimes are presented. The lifetimes were measured for two different temperatures, viz. 363 and 420 K. In order to check the lifetime measured values, measurements using the well-known open circuit voltage decay (OCVD) technique are compared with the OCCD-measured values. The results are shown in Fig. 11. A sample current of 0.5 A gave an injection level of approximately 6×10^{15} cm^{-3} in this set of measurements. In accordance with previous investigations,[11] the OCVD measurements gave somewhat higher values than the OCCD measurements. This discrepancy in lifetimes values between measurement techniques is partly due to the fact that the OCVD technique gives an average measure of the lifetime whereas local lifetime values are obtained by the OCCD technique. In addition, the temperature range of the OCVD technique was extended down to 200 K. From Fig. 11 a good agreement between the lifetime-measurement techniques is observed, specifically for measurements above room temperature. However, the electron capture-coefficient temperature dependence, $c_n(T)$, proposed in this paper seems to be in parity with the OCVD lifetime values for temperatures below 300 K as well.

IV. DISCUSSION

The capture coefficients for electrons and holes for the recombination center associated with the $E4$ defect level, $E_c - 0.421$ eV, is shown experimentally to govern the

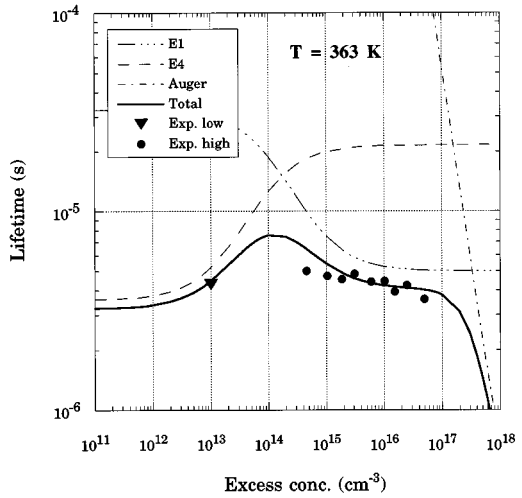

FIG. 7. The total effective lifetime of diode 1 vs excess carrier concentration at 363 K. The markers, (▼) and the (●) represent the measured low-, and the high-injection lifetime respectively. The solid line (—) shows the computed total effective lifetime from the DLTS data.

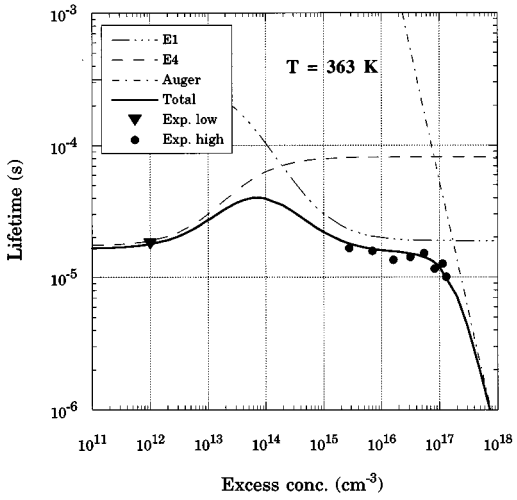

FIG. 9. The total effective lifetime of diode 2 vs excess carrier concentration at 363 K. The markers, (▼) and the (●) represent the measured low-, and high-injection lifetime respectively. The solid line (—) shows the computed total effective lifetime.

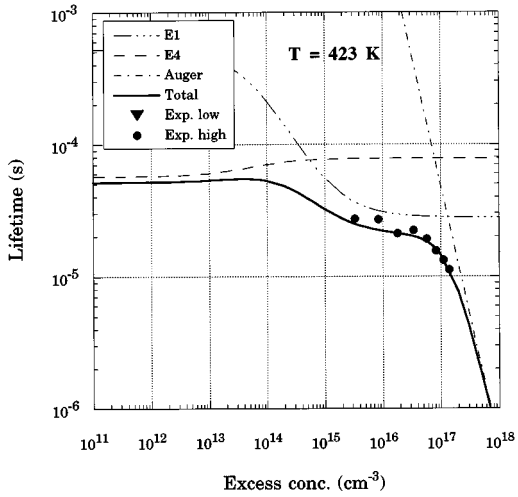

FIG. 10. The total effective lifetime of diode 2 vs excess carrier concentrations at 423 K. The markers, (▼) and the (●) represent the measured low-, and the high-injection lifetime respectively. The solid line (—) shows the computed total effective lifetime.

low-injection lifetime. Among others, Watkins *et al.*[14] and Brotherton *et al.*[15] correlated this center to be a single-negatively charged state of the divacancy. Moreover, in Ref. 15 the authors proposed the existence of two dominating recombination centers viz. $E1$ and $E4$. The model proposed by Hallén *et al.* which is obtained using the DLTS technique gives further strength to this theory.[10] The temperature dependence of the capture coefficients which governs the lifetime temperature dependence is showing very good agreement with experimental data obtained in this work. The reason for this is that the recombination parameters of the $E4$ defect level is measured close to room temperature by a DLTS setup ranging in the temperature interval from 182 to 266 K. It should be kept in mind that an important parameter

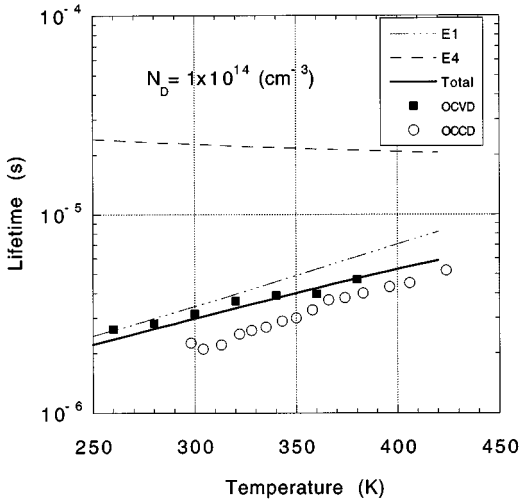

FIG. 11. The total effective lifetime of diode 1 vs temperature at a medium injection level of about 6×10^{15} cm^{-3}. The experimental results are obtained according to the OCVD (■), and the OCCD (○) techniques.

in the calculation of the low-injection lifetime is the temperature dependence of the Fermi-level position in the band diagram.

The $E1$ level correlated to the vacancy-oxygen complex by Refs. 15 and 16 is measurable by means of the present DLTS equipment in the temperature interval of 80–108 K.[10] Thus, the capture-coefficient temperature dependence has to be extrapolated in order to investigate the influence at far higher temperature values. In the present work it is shown that such extrapolation are hazardous to rely on. Hence, an indirect correction of the electron capture cross section, σ_n, of the $E1$ defect level between room temperature and 420 K was performed using experimental data, cf. Fig. 6. On the other hand, the deviation between capture cross sections in the two temperature intervals (80–108 K) and (300–420 K) may be differing capture mechanisms. However, in the low-injection mode, this defect level is less important due to its position in the band diagram ($E_c-0.164$ eV) in relation to the quasi-Fermi level. As the diode goes into the high-injection mode, the electron quasi-Fermi level approaches this defect level which is becoming increasingly efficient, a strong influence on the high-injection lifetime.

From the DLTS measurements, a defect level located at the position $E_C-0.35$ eV ($E6$) is also visible in Fig. 3, i.e. the response peak located directly to the left of the $E4$ response peak. This defect level was also observed by Evwaraye *et al.*[11] In Ref. 11, the authors reported that $E6$ is not present as a recombination center in non-annealed samples. On the other hand, the longer annealing times and the higher annealing temperatures was used, the larger the peak in the DLTS spectrum becomes. Simultaneously, the $E4$ DLTS peak is reduced. This indicates that the $E6$ level may be of importance for samples of different annealing processes than the one used in this work. A more extensive investigation of the behavior of these two centers in relation to the annealing time and temperature should be done.

In Fig. 3, a double-negatively charged state of the divacancy located at $E_c-0.225$ eV ($E2$) in the band diagram is also present. The efficiency of this center is also negligible due to its relatively slow recombination rate. Furthermore, the low $E2$ trap concentration and position in the band diagram tend to decrease the possible influence on the high-injection and low-injection lifetimes.

In Figs. 4, 5, and 7–10, the Auger-recombination influence on the lifetime is also included. However, in this paper Auger effects are not put in focus. Another work concerning the temperature and excess-carrier dependence of the Auger recombination process will be published.

Recently, multilevel recombination-center device simulator tools have been developed.[17] Nevertheless, accurate input data are needed in order to achieve reliable results form such tools. For the calculation of the total lifetime variations with temperature, it is not sufficient to input the temperature variation of the recombination capture coefficients given in this work. It is also necessary to know the trap concentration—a value dependent on the electron-irradiation flux and annealing process used. Such data can be achieved using e.g., DLTS facilities. A set of parameters for a simplified

calculation of the lifetime including the temperature dependence is presented here.

The temperature dependence of the electron and the hole lifetimes for the $E4$ recombination center are:

$$\tau_{n_0,E4} = \tau_{n_0} \times \left(\frac{T}{300} \right)^{-0.4} \tag{9}$$

and

$$\tau_{p_0,E4} = \tau_{p_0} \times \left(\frac{T}{300} \right)^{0.3}, \tag{10}$$

where τ_{n_0} and τ_{p_0} are the electron and hole lifetimes, respectively, at room temperature and the temperature, T, is given in degrees Kelvin.

The ratio between minority and majority carrier lifetime at room temperature is

$$\frac{\tau_{n_0,E4}}{\tau_{p_0,E4}} \approx 6.8\,. \tag{11}$$

This value should be compared to the commonly used 4.42 proposed by Ref. 6. Recently, this value was corrected by Yahata *et al.*[18] who gave a value between 7 and 9 for electron-irradiated samples, which is in agreement with Ref. 10.

The electron and hole lifetimes for the $E1$ recombination center are:

$$\tau_{n_0,E1} = \tau_{n_0} \times \left(\frac{T}{300} \right)^{2.4} \tag{12}$$

and

$$\tau_{p_0,E1} = \tau_{p_0} \times \left(\frac{T}{300} \right)^{-0.7}. \tag{13}$$

The ratio between lifetimes at room temperature is

$$\frac{\tau_{n_0,E1}}{\tau_{p_0,E1}} \approx 50. \tag{14}$$

The ratio between the majority and minority lifetimes with respect to the $E4$ and $E1$ traps are:

$$\frac{\tau_{n_0,E4}}{\tau_{n_0,E1}} \approx 6.2, \qquad \frac{\tau_{p_0,E4}}{\tau_{p_0,E1}} \approx 45.6. \tag{15}$$

For the sake of applications, simulated and measured data of real semiconductor devices, e.g., electron-irradiated gate turn-off thyristors (GTOs) and diodes, will be compared as regards static and dynamic electrical characteristics as well as excess-carrier distributions. Such a comparison will be presented in a future paper by the authors, and will act as a synthesis of presented and prospected results of fundamental physical recombination effects.

V. CONCLUSIONS

Two recombination centers seem to be involved in and dominating the SRH lifetime. These recombination centers act predominantly at different injection levels. In this respect, the $E4$ recombination center, which is associated with a single-negatively charged divacancy state, is dominating the low-injection lifetime. The high-injection lifetime is dominated by the $E1$ recombination center which is associated with a vacancy-oxygen complex.

In specific cases of the annealing process, another recombination center may occur while the $E4$ center is weakening.

In this article, defect-related models with respect to temperature and injection level are proposed in order to facilitate for accurate simulations of semiconductor device behavior.

ACKNOWLEDGMENTS

The authors would like to thank Dr. Mietek Bakowski, now affiliated with the Industrial Microelectronics Center (IMC), Kista-Stockholm, Sweden, who at the time was involved in the processing of the samples at ABB Drives in Västerås, Sweden. Dr. Anders Hallén, Uppsala University, is also gratefully acknowledged for his concern in this work and putting up facilities for the DLTS investigations. Dr. Ferenc Masszi, Uppsala University and Dr. Mats Rosling, Micronic Laser System AB, Sweden are also acknowledged for their concern in this work.

[1] H. Bleichner, E. Nordlander, G. Fiedler, and P. A. Tove, Solid-State Electron. **29**, 779 (1986).
[2] M. Rosling, H. Bleichner, M. Lundqvist, and E. Nordlander, Solid-State Electron. **35**, 1223 (1992).
[3] P. Jonsson, M. Isberg, M. Rosling, H. Bleichner, and E. Nordlander, Solid-State Electron. (submitted).
[4] L. W. Davies, Proc. IEEE **51**, 1637 (1963).
[5] D. V. Lang, J. Appl. Phys. **45**, 30 (1974).
[6] B. J. Baliga, *Modern Power Devices* (Wiley, New York, 1987).
[7] O. Engström and A. Alm, Solid-State Electron. **21**, 1571 (1978).
[8] L. C. Kimerling, Inst. Phys. Conf. Ser. **31**, 221 (1977).
[9] L. C. Kimerling, P. Blood, and W. M. Gibson, Inst. Phys. Conf. Ser. **46**, 273 (1979).
[10] A. Hallén, N. Keskitalo, F. Masszi, and V. Nágl, J. Appl. Phys. **8**, 3906 (1996).
[11] A. O. Evwaraye and B. J. Baliga, J. Electrochem. Soc. **124**, 913 (1977).
[12] M. Rosling, H. Bleichner, and E. Nordlander, Symposium on Materials and Devices for Power Electronics, 1991 Proc. MADEP '91, pp. 59–64.
[13] M. A. Green, J. Appl. Phys. **67**, 2944 (1990).
[14] G. D. Watkins and J. W. Corbett, Phys. Rev. **138**, A 543 (1965).
[15] S. D. Brotherton and P. Bradley, J Appl. Phys. **53**, 5720 (1982).
[16] G. D. Watkins and J. W. Corbett, Phys. Rev. **121**, 1001 (1961).
[17] Medici Version 2.0
[18] A. Yahata, Y. Yamaguchi, and A. Nakagawa, IEEE Trans. Electron Devices **39**, 1003 (1992).